Vol. 122: 1–11, 2016
doi: 10.3354/dao03059

DISEASES OF AQUATIC ORGANISMS
Dis Aquat Org

Published November 22

Genetic characterization of esocid herpesvirus 1 (EsHV1)

Jared T. Freitas[1], Kuttichantran Subramaniam[2], Karen L. Kelley[3], Susan Marcquenski[4], Joseph Groff[5], Thomas B. Waltzek[2,*]

[1]College of Agriculture and Life Science, University of Florida, Gainesville, FL 32610, USA

[2]Department of Infectious Diseases and Pathology, College of Veterinary Medicine, University of Florida, Gainesville, FL 32610, USA

[3]Electron Microscopy Core, Interdisciplinary Center for Biotechnology Research, University of Florida, Gainesville, FL 32611, USA

[4]Bureau of Fisheries Management, Wisconsin Department of Natural Resources, 101 South Webster Street, Box 7921, Madison, WI 53707, USA

[5]College of Veterinary Medicine, University of California Davis, Davis, CA 95616, USA

ABSTRACT: Blue spot disease, believed to be caused by esocid herpesvirus 1 (EsHV1), has been observed in wild northern pike *Esox lucius* in a number of cold-water locations, including the northern USA, Canada, and Ireland. In the spring of 2014, a northern pike was caught in Wisconsin displaying the characteristic bluish-white circular plaques on the dorsum and fins. Microscopic examination of hematoxylin and eosin-stained sections of the proliferative cutaneous lesions revealed a focally extensive abundance of panepidermal, megalocytic keratinocytes with karyomegaly. Enlarged nuclei stained basophilic, and an abundance of coarse eosinophilic granules were observed in the expanded cytoplasm. Transmission electron microscopy revealed aggregates of enveloped virus particles with electron-dense, hexagonal nucleocapsids surrounded by a uniformly staining ellipsoidal tegument layer within cytoplasmic vacuoles of megalocytic epidermal cells. More than 7000 bp of the EsHV1 genome were sequenced from infected skin tissues. Phylogenetic and phenetic analyses, based on the partial DNA-dependent DNA polymerase and terminase gene sequences, revealed EsHV1 forms a novel branch within the family *Alloherpesviridae* as the sister group to the clade that includes members of the genera *Ictalurivirus* and *Salmonivirus*. The gross, microscopic, and ultrastructural lesions reported in our study were identical to previous reports of blue spot disease in northern pike; however, here we provide the first molecular evidence supporting EsHV1 as a new species in the family *Alloherpesviridae*.

KEY WORDS: *Esox lucius* · Northern pike · Blue spot disease · *Alloherpesviridae*

INTRODUCTION

Northern pike *Esox lucius* display a circumpolar distribution, including northern Europe, Russia, Canada, and the northern USA (Craig 2008, 2013). They serve as apex predators in lakes and rivers, and thus play an important role in regulating the population dynamics of their fish prey (Craig 2008, 2013). Northern pike reach upwards of 20 kg in weight and the combination of their large size (records of up to 155 cm total length) and aggressive fighting behavior when caught makes them a favorite among sport fishermen in Canada and the northern USA (Craig 2008, 2013). The economic importance of the northern pike sport fishery is evident from the 2013 catch records, in which 22 893 tons were landed globally (FAO 2015).

*Corresponding author: tbwaltzek@ufl.edu

A variety of viruses have been described from wild and cultured northern pike. The first discovered was the pike fry rhabdovirus that induces lethal systemic disease in cultured fry and fingerlings in Europe (de Kinkelin et al. 1973). Several strains of a second rhabdovirus, viral hemorrhagic septicemia virus, have been associated with epizootics in wild and cultured stocks of northern pike in Europe (Meier & Jørgensen 1980, Enzmann et al. 1993), and more recently in wild northern pike within Lake Michigan (Faisal et al. 2012). The first DNA virus detected in wild northern pike displaying proliferative lesions of the skin and fins was the iridovirus lymphocystis (Amin 1979). Histological examination revealed hypertrophy of subcutaneous fibroblasts surrounded by a hyaline capsule (Amin 1979). Shortly thereafter, another hyperplasia-inducing viral disease of the skin and fins in wild Canadian northern pike was reported (Yamamoto et al. 1984). In one manifestation, fish displayed raised, bluish-white, granular growths with a diameter of 3 to 10 mm and a thickness of up to 0.25 mm. Microscopic examination identified megalocytic epidermal cells with dark-staining karyomegalic nuclei and an expanded cytoplasm containing abundant eosinophilic granules. Transmission electron microscopy (TEM) revealed herpesvirus particles consisting of naked icoasahedral nucleocapsids (100 to 110 nm in diameter) within the nucleus and aggregations of enveloped, tegument-wrapped nucleocapsids within cytoplasmic vacuoles. Based on the bluish gross skin lesions, the condition was referred to as blue spot disease, and the presumptive causative agent was named esocid herpesvirus 1 (EsHV1) after the host, which is a member of the family Esocidae. The prevalence of blue spot disease from 1984 to 1991 was found to be as high as 34% in northern pike and 29% in muskellunge *Esox masquinongy* populations in northern Wisconsin (Margenau et al. 1995). The latest detection in wild northern pike in Ireland confirms the widespread distribution of blue spot disease (Graham et al. 2004).

The order *Herpesvirales* is split into 3 families: *Herpesviridae* (includes mammalian, avian, and reptilian herpesviruses), *Malacoherpesviridae* (includes mollusk herpesviruses), and *Alloherpesviridae* (includes fish and amphibian herpesviruses). According to the most recent update by the International Committee on the Taxonomy of Viruses (ICTV), there are 12 valid species organized into 4 genera within the family *Alloherpesviridae* (Davison et al. 2009). *Ictalurid herpesvirus 1*, *Ictalurid herpesvirus 2*, and *Acipenserid herpesvirus 2* are grouped into the genus *Ictalurivirus*; *Salmonid herpesvirus 1*, *Salmonid herpesvirus 2*, and *Salmonid herpesvirus 3* are grouped in the genus *Salmonivirus*; *Cyprinid herpesvirus 1*, *Cyprinid herpesvirus* 2, *Cyprinid herpesvirus* 3, and *Anguillid herpesvirus 1* are grouped into the genus *Cyprinivirus*; and *Ranid herpesvirus 1* and *Ranid herpesvirus 2* are grouped into the genus *Batrachovirus*.

Despite having been detected multiple times in wild northern pike from North America and Europe displaying the classic disease presentation, sequence data confirming EsHV1 as a member of the family *Alloherpesviridae* is lacking. In this investigation, we compared the lesions of a northern pike exhibiting signs of blue spot disease to previous studies, and determined the relationship of the viral etiological agent in this host to other known alloherpesviruses based on phylogenetic and phenetic analyses of the partial DNA polymerase and terminase genes.

MATERIALS AND METHODS

Sample collection, histopathology, and TEM

In April 2014, a gravid female northern pike was caught using fyke nets in Lower Mud Lake (Dane County, WI). This was done during the spawning season to collect eggs for state fish hatcheries and as part of a routine fish health assessment conducted by the Wisconsin Department of Natural Resources (Madison, WI). The typical gross lesions of blue spot disease, indicated by small bluish-white circular plaques, were present on the dorsum and fins. The fish was euthanized, bagged, and transported on ice to the WI Department of Natural Resources Fish Health Laboratory for necropsy and tissue collection. The proliferative lesions of the skin and fins were removed from the fish and fixed in Davidson's fixative for 24 h, transferred to 70% ethanol, and processed by standard histological methods for paraffin-embedded tissues (Humason 1979) at the Wisconsin Veterinary Diagnostic Laboratory (Madison, WI). Paraffin-embedded blocks were cut at 5 µm, stained with hematoxylin and eosin, and examined by light microscopy. For TEM, proliferative skin lesions were fixed in Karnovsky's fixative, refrigerated overnight, post-fixed in 2% osmium tetroxide, dehydrated, and embedded in Polybed 810 (Polysciences) at the University of Wisconsin-Madison Electron Microscope Facility (Madison, WI), before being transferred to the Electron Microscopy Core, Interdisciplinary Center for Biotechnology Research, University of Florida. Ultra-thin sections at 80 to 120 nm were collected on

carbon-coated Formvar copper 100 mesh grids, and post-stained with 2% aqueous uranyl acetate and Reynold's lead citrate. Sections were viewed on a Hitachi H-7000 transmission electron microscope (Hitachi High Technologies America). The digital images were acquired with a Veleta 2k × 2k camera and iTEM software program (Olympus Soft-Imaging Solutions).

DNA extraction and PCR amplification

A section of skin displaying multiple proliferative lesions consistent with blue spot disease was sent frozen on dry ice from the Wisconsin Department of Natural Resources to the Wildlife and Aquatic Veterinary Disease Laboratory (Gainesville, FL). DNA from the skin sample was extracted using a Maxwell 16 tissue DNA purification kit (Promega) according to manufacturer's instruction. Nucleic acid quality and concentration was quantified using a NanoDrop 8000 spectrophotometer (Thermo Scientific).

A degenerate conventional PCR assay (Hanson et al. 2006) targeting a conserved region of the DNA-dependent DNA polymerase of large DNA viruses (open reading frame 57 [ORF57] in *Ictalurid herpesvirus 1* [IcHV1]) was employed to confirm the presence of an alloherpesvirus (Table 1). Conventional PCR relying on a previously published degenerate primer set (Doszpoly & Shchelkunov 2010) that targets a conserved region of the first exon of the alloherpesvirus terminase (ORF62 in IcHV1), and a new primer set designed against the second exon, were employed to amplify downstream regions of the alloherpesvirus genome (Table 1). In an effort to amplify the region between the DNA polymerase and first exon of the terminase, a long PCR was performed using specific primers generated from the aforementioned PCR and sequencing reactions (Table 1).

The 50 µl conventional PCR reaction mixtures consisted of 33.75 µl molecular grade water, 5 µl 10× PCR buffer, 2 µl 50 mM $MgCl_2$, 1 µl 10 mM dNTPs, 2.5 µl 20 mM forward and reverse primers, 0.25 µl Platinum *Taq* DNA polymerase (Invitrogen), and 3 µl DNA template. An initial denaturation step of 95°C for 5 min was followed by 50 cycles of a 95°C denaturation step, a 48°C annealing step, and a 72°C extension step, each run for 1 min, and a final extension step at 72°C for 10 min. PCR products were subjected to electrophoresis on a 1% agarose gel. Bands of the correct size were extracted using the QIAquick gel extraction kit (Qiagen) and the purified DNA was sent to the University of Florida's Interdisciplinary Center of Biotechnology Research (ICBR) for Sanger sequencing in both directions on an ABI 3130 platform (Applied Biosystems).

The long PCR reaction was carried out using a Takara Clontech high fidelity PrimeSTAR GXL DNA polymerase kit as specified by the manufacturer. The PCR was conducted using the EsHV1POLIN/EsHV1TERMIN primers (Table 1). The reaction consisted of an initial denaturation step of 98°C for 5 min followed by 35 cycles of a 98°C denaturation step for 10 s, a 55°C annealing step for 15 s, a 68°C extension step for 8 min, and a final extension step at 68°C for 7 min. The PCR product was electrophoresed, purified, and sequenced (as described above) employing a primer walking strategy to bridge the gap between the genes coding for the DNA polymerase and the first exon of the terminase.

Genome annotation, phenetic analysis, and phylogenetic analysis

CLC Genomics Workbench v.7.5 software was used to edit sequencing reads and remove primer sequences. The edited sequence reads were then

Table 1. Primer pairs used for PCR of the DNA polymerase and terminase genes. The listed amplicon size excludes the primers

Primer pair	Primer sequence (5′ to 3′)	Gene of interest	Amplicon size	Reference
CONDNAPOLF	CGGAATTCTAGAYCNWSNYTNTAYCC	Polymerase	442	Hanson et al. (2006)
CONDNAPOLR	CCCGAATTCAGATCNGTRTCNCCRTA			
ORF62F	TTYCARBTNGARYTNATGMGNGG	Terminase exon 1	259	Doszpoly & Shchelkunov (2010)
ORF62R	TGNGCYTGNACNACDATNTCDAT			
EsHV1TERMF	ATCACGACAAACTCGCATCC	Terminase exon 2	643	This study
EsHV1TERMR	TGGATTTTGTGTTCCCCAAT			
EsHV1POLIN	ACCCCTAGCTCCCTTAGACG	Polymerase Terminase exon 1	6776	This study
EsHV1TERMIN	GTGTAGTTCCGCGCGTATATC			

assembled in CLC to generate a single contig bridging the gap between the genes coding for the DNA polymerase and the first exon of the terminase. The contig ORFs were predicted using CLC, and intron–exon boundaries were determined based on previously established guidelines for alloherpesviruses (Davison 1998). The resulting ORFs were then used as queries for BLASTX searches (Altschul et al. 1997). The BLASTX results were used to find appropriate alloherpesviruses for the phylogenetic analysis (Table 2).

Table 2. GenBank accession numbers for the alloherpesvirus DNA polymerase and terminase (exon 2) gene sequences used in the phylogenetic and phenetic analyses

Species name (virus abbreviation)	DNA polymerase	Terminase exon 2
Ranid herpesvirus 2 (RaHV2)	ABG25576.1	ABG25669.1
Ranid herpesvirus 1 (RaHV1)	AAD12269.1	ABG25767.1
Acipenserid herpesvirus 1 (AciHV1)	ABS18306.1	ABQ10595.1
Cyprinid herpesvirus 3 (CyHV3)	AAX53082.1	BAF48846.1
Cyprinid herpesvirus 2 (CyHV2)	AKC02025.1	AFJ20476.1
Cyprinid herpesvirus 1 (CyHV1)	AAX53084.1	AFJ20337.1
Anguillid herpesvirus 1 (AngHV1)	ADA57818.1	ACD84540.1
Salmonid herpesvirus 4 (SalHV4)	AGB07609.1	AGB07606.1
Salmonid herpesvirus 3 (SalHV3)	ACD84539.1	ACD84548.1
Salmonid herpesvirus 2 (SalHV2)	ACD84537.1	ACD84546.1
Salmonid herpesvirus 1 (SalHV1)	ACD84535.1	ACD84543.1
Ictalurid herpesvirus 2 (IcHV2)	ACZ55873.1	NP_041153.2
Ictalurid herpesvirus 1 (IcHV1)	AAA88160.2	ACD84542.1
Acipenserid herpesvirus 2 (AciHV2)	ACZ55868.2	ABQ10594.1
Esocid herpesvirus 1 (EsHV1)	This study	This study

Sequence alignments were performed in MAFFT 5.8 using default parameters (Katoh et al. 2005). Phenetic analyses of the aligned partial amino acid (AA) sequences of the DNA polymerase and terminase (exon 2) genes were compared using the sequence demarcation tool independently to quantitatively evaluate the identity of EsHV1 to other members of the family *Alloherpesviridae* (Muhire et al. 2014). The aligned partial DNA polymerase and terminase (exon 2) genes sequences were then concatenated in the Geneious (Biomatters) software package. The final dataset contained 261 AA characters (including gaps) and was imported into MEGA6 to generate a maximum likelihood tree (JTT evolutionary model, 1000 bootstraps).

RESULTS

Gross, microscopic, and ultrastructural pathology

Gross proliferative skin lesions were apparent on the dorsum and fins. These circular raised lesions were granular and bluish-white in appearance, with a diameter between 5 and 12 mm (Fig. 1A). Microscopic examination of the cutaneous lesions revealed a focally extensive abundance of panepidermal, megalocytic, epidermal cells with karyomegaly that were presumed to represent transformed keratinocytes (Fig. 1B). The enlarged nuclei generally had spherical to slightly elongated profiles with a variable central to peripheral intracellular location, and were composed of a homogeneous, flocculent to fine granular, basophilic nucleoplasm (Fig. 1C). The nuclear membranes were absent or otherwise not apparent, although fine, slightly irregular, intact, internal membranous structures often occurred within the nucleoplasm. In contrast, the cytoplasm contained an abundance of coarse eosinophilic granules (Fig. 1C). The megalocytic epidermal cells (n = 32) were 57.5 to 150 µm in diameter, whereas the nuclei were 32.5 to 60 µm in diameter, which resulted in a nuclear to cytoplasmic ratio of 0.30–0.85. Inflammation was not observed in the affected integument.

TEM revealed abundant virus particles in various stages of development within megalocytic cells (Figs. 2 & 3). Within the nucleus, naked hexagonal shaped capsids were observed in various states of morphogenesis, including immature forms appearing as empty shells (A-capsids), maturing forms arranged in arrays (B-capsids), and more mature forms containing an electron-dense nucleoid (C-capsids) (Figs. 2 & 3A). Maturing nucleocapsids were observed budding into and within the perinuclear space as they traversed from the nucleus into the cytoplasm (Fig. 2). Although single enveloped virus particles were observed in the cytoplasm, the vast majority occurred as aggregates embedded within a finely granular matrix and bounded by an outer membrane (i.e. cytoplasmic vacuoles). The cytoplasmic vacuoles varied in size, containing from as few as 1 virus particle up to approximately 50 particles in cross-section (Fig. 3B). The mature virus particles displayed electron-dense hexagonal nucleocapsids surrounded by a uniformly staining ellipsoidal tegument layer and a transparent envelope (Fig. 3C). The mean diameter of the nucleocapsids was 91.32 nm (n = 20, SD = 2.64 nm) from opposite vertices and 86.42 nm (n = 20, SD = 3.23 nm) from opposite faces.

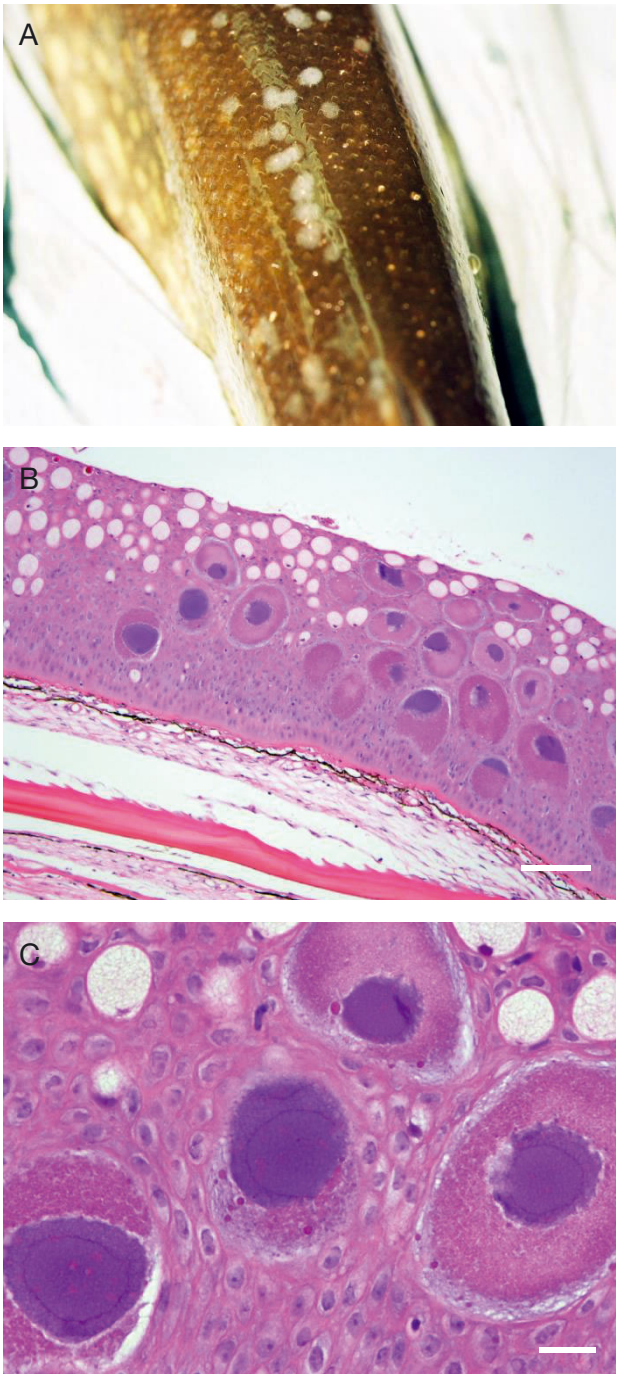

Fig. 1. *Esox lucius*. (A) Gross photograph of a wild northern pike displaying the characteristic bluish-white circular proliferative lesions on the dorsal epidermis characteristic of blue spot disease. (B) Microscopic examination of the cutaneous lesions illustrating megalocytic epidermal cells with karyomegaly. Hematoxylin and eosin (H&E) stain. Scale bar = 100 µm. (C) The enlarged nuclei contain a homogeneous, flocculent to fine granular, basophilic nucleoplasm with internal membranous structures. The cytoplasm contains an abundance of coarse eosinophilic granules. H&E stain. Scale bar = 20 µm

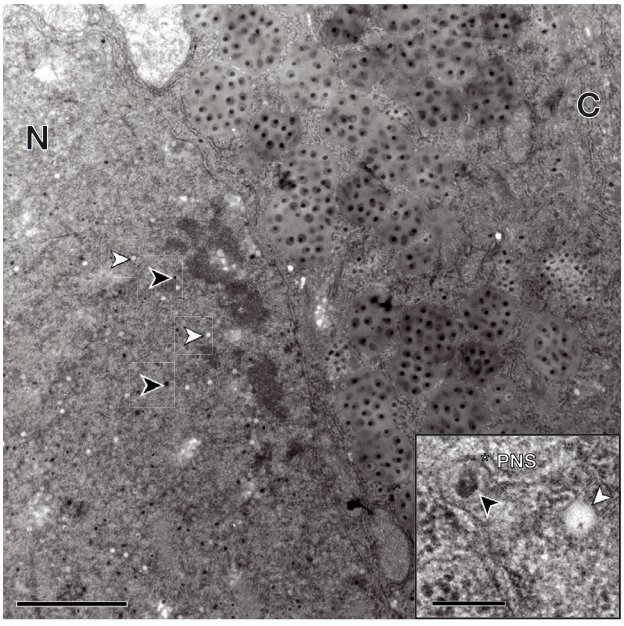

Fig. 2. *Esox lucius*. Transmission electron photomicrograph of a megalocytic epidermal cell illustrating the boundary between the nucleus (N) and the cytoplasm (C). A-capsids (white arrowheads) and C-capsids (black arrowheads) are present within the nucleus. Scale bar = 2 µm. Inset: nucleocapsid acquiring an envelope as it buds into the perinuclear space (PNS) as indicated by the black arrowhead, and an A-capsid indicated by a white arrowhead. Scale bar = 200 nm

Genome annotation, phenetic analysis, and phylogenetic analysis

The conventional PCRs targeting the EsHV1 DNA polymerase and terminase (exons 1 and 2) genes produced amplicons of the expected sizes (Table 1). Sequencing reactions for the second exon of the terminase gene resulted in 643 bp of the EsHV1 genome and were deposited into GenBank under accession no. KX385272. The EsHV1 sequence reads generated by the long PCR and primer walking strategy assembled into a single 6776 bp contig. Combining the sequence generated from the degenerate and long PCR reactions resulted in a single 7086 bp contig with 4× sequence coverage, which was deposited into GenBank under accession no. KX198667. The EsHV1 contig encoded (1) partial DNA polymerase (ORF57 in IcHV1), (2) full-length major envelope protein (ORF59 in IcHV1), (3) full-length hypothetical gene (ORF60 in IcHV1), (4) full-length hypothetical gene (ORF61 in IcHV1), and (5) partial exon 1 of the terminase gene (ORF62 in IcHV1). Comparison of the partial EsHV1 genome to the homologous regions in the genomes of IcHV1 (positions 75904 to

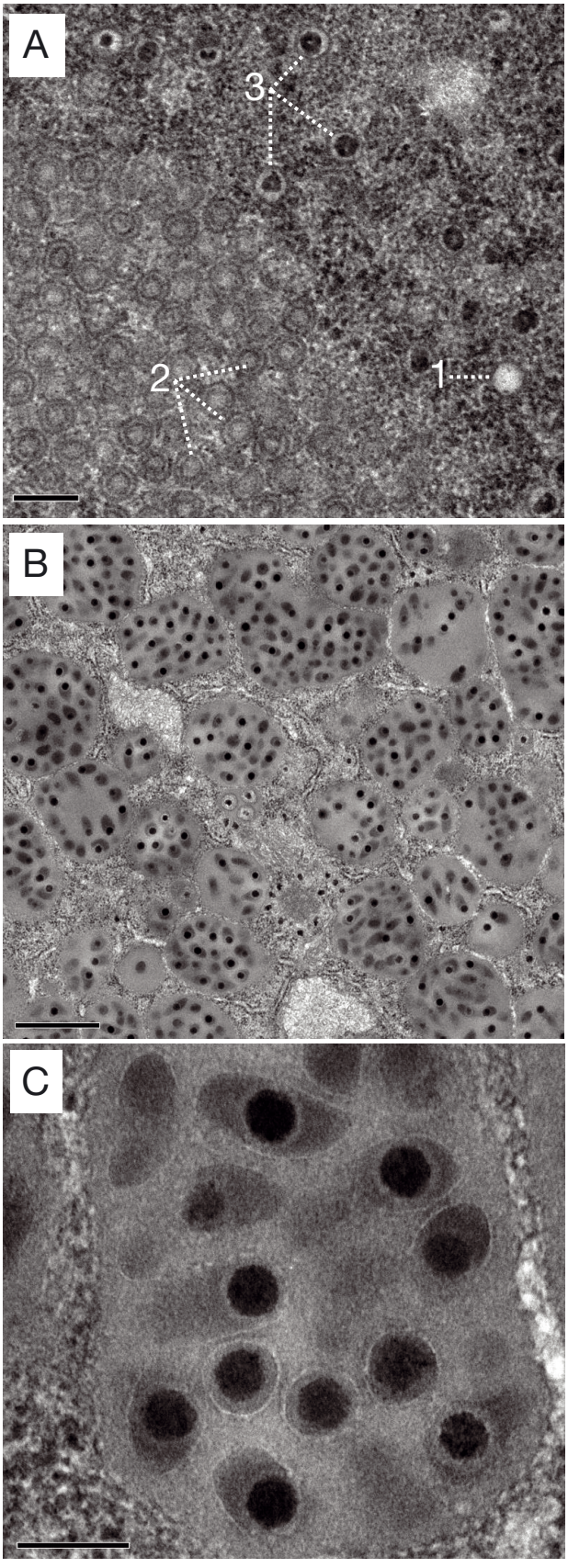

Fig. 3. *Esox lucius*. (A) Transmission electron photomicrograph illustrating A-capsids (1), an array of B-capsids (2), and C-capsids (3) within the nucleus. Scale bar = 200 nm. (B) Higher magnification of the expansive network of cytoplasmic vacuoles containing mature virus particles. Scale bar = 1 µm. (C) Mature virus particles composed of an electron-dense hexagonal nucleocapsid surrounded by a uniformly staining ellipsoidal tegument layer and a transparent envelope. Scale bar = 200 nm

82504; GenBank accession no. M75136.2), IcHV2 (positions 1309 to 7982; GenBank accession no. FJ815290.1), and AciHV2 (positions 42216 to 48832; GenBank accession no. FJ815289.2) revealed complete collinearity among these ictaluriviruses (Fig. 4). The EsHV1 DNA polymerase sequence was predicted to encode an intron from positions 798 to 876 similar to IcHV1, IcHV2, and AciHV2 (Fig. 4).

The phenetic analyses of the partial EsHV1 DNA polymerase and terminase (exon 2) gene sequences ranged from 33.3 to 45.2% and 34.4 to 52.2% identities to other alloherpesviruses, respectively (Table 3). The highest identities were observed with alloherpesviruses from salmonid, ictalurid, and acipenserid (AciHV2) fishes. The maximum likelihood analysis of the concatenated partial DNA polymerase and terminase gene sequences produced a well-resolved and supported tree (Fig. 5). Similar to the phenetic analyses, EsHV1 grouped closest to alloherpesviruses infecting salmonid, ictalurid, and acipenserid (AciHV2) fishes.

DISCUSSION

The size (5 to 12 mm), composition (granular plaques), and color (bluish-white) of the proliferative cutaneous lesions reported here (Fig. 1A) are nearly identical to the previous descriptions of blue spot disease in northern pike and muskellunge (Yamamoto et al. 1984, Margenau et al. 1995, Graham et al. 2004). Herpesviruses that induce proliferative cutaneous lesions have been described from a wide variety of both cultured and wild freshwater and marine fishes (reviewed in Wolf 1988, Anders & Yoshimizu 1994). Infected fish have been described as if they have been dipped in candlewax resulting from the focal, multifocal to coalescing, or diffuse epithelial hyperplasia that sometimes progresses to neoplasia (e.g. papilloma). Hyperplastic skin lesions similar to EsHV1 (i.e. focal or multifocal to coalescing hyperplasia) of a known or likely herpesvirus etiology include the well-studied carp pox agent, formally

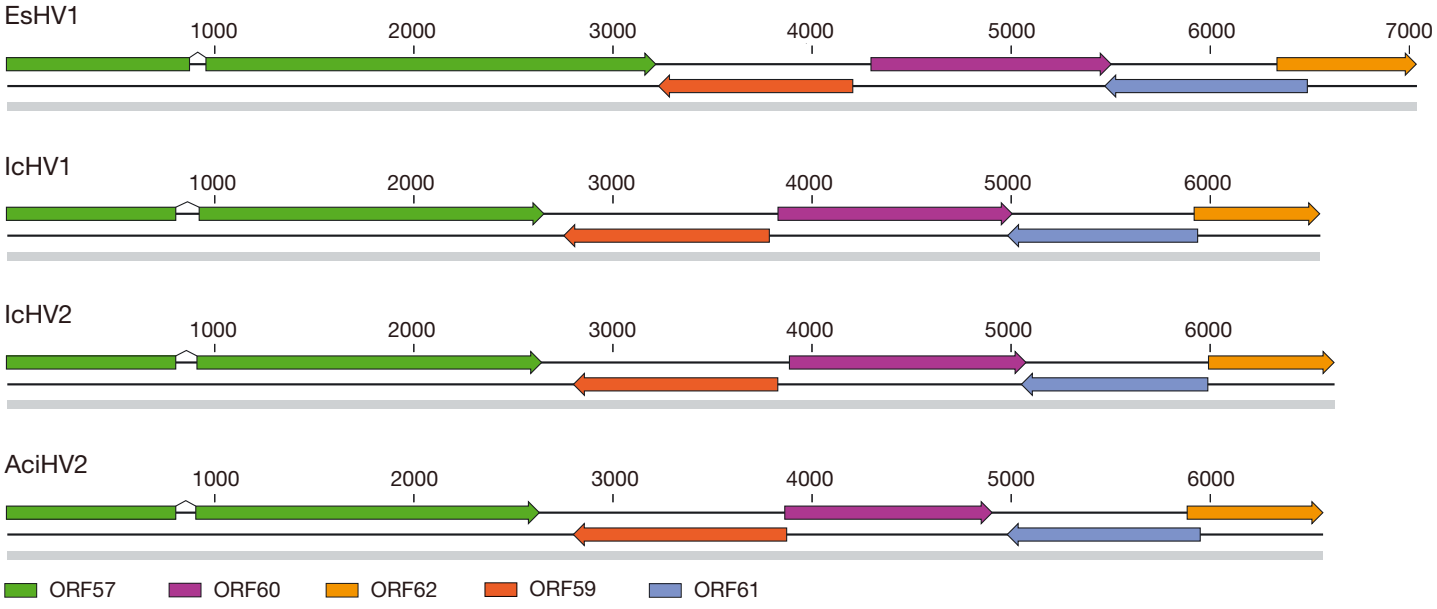

Fig. 4. Comparative partial genomic organization among EsHV1, IcHV1, IcHV2, and AciHV2. ORFs are indicated by colored arrows and identified in the key. See Table 2 for virus abbreviations

known as *Cyprinid herpesvirus 1* (CyHV1) that infects common carp varieties. Herpesviruses associated with proliferative cutaneous lesions have been observed in smooth dogfish *Mustelus canis* (Wolke & Murchelano 1976), Pacific cod *Gadus macrocephalus* (McArn et al. 1978), sheatfish *Silurus glanis* (Békési et al. 1984), walleye *Sander vitreus* (Kelly et al. 1983), European smelt *Osmerus eperlanus* (Anders & Möller 1985), golden ide *Leuciscus idus* (McAllister et al. 1985), Japanese flounder *Paralichthys olivaceus* (Iida et al. 1989), Atlantic salmon *Salmo salar* (Shchelkunov et al. 1992), and rainbow smelt *Osmerus mordax* (Morrison et al. 1996). Although viral challenge studies have proven CyHV1 and some strains of salmonid herpesvirus 2 can induce proliferative lesions (e.g. papillomas) in their respective hosts, other investigations have simply noted the presence of alloherpesvirus particles within proliferating tissues. The isolation of EsHV1 and the other aforementioned herpesviruses would permit challenge studies to establish whether the observed proliferative cutaneous lesions are viral induced. Furthermore, the molecular mechanism(s) that alloherpesviruses utilize to induce epithelial proliferative lesions in their respective hosts remain virtually unknown. Interestingly, the genomic sequencing of CyHV1 revealed a family of genes that encode a JunB transcription factor that may be involved in oncogenesis (Davison et al. 2013).

The EsHV1-induced microscopic lesions in this presented case consisted of megalocytic epithelial cells with enlarged basophilic-staining nuclei and a granular eosinophilic-staining cytoplasm (Fig. 1B,C) similar to previous reports of blue spot disease in northern pike (Yamamoto et al. 1984, Margenau et al. 1995, Graham et al. 2004). Other epitheliotropic alloherpesviruses of marine fishes including turbot (McArn et al. 1978, Hellberg et al. 2002) and Pacific (Richards & Buchanan 1978) and Atlantic cod (Marcos-Lopez et al. 2012) induce similar microscopic lesions in the integument and gills. However, the turbot herpesvirus is differentiated from the others by the fact that the karyomegalic epithelial cells may contain multiple nuclei thought to arise from the fusion of adjacent cells in the formation of syncytia (Buchanan et al. 1978, Richards & Buchanan 1978).

The ultrastructural findings are consistent with typical herpesvirus virion morphogenesis including the observation of (1) naked hexagonal shaped nucleocapsids in various stages of development within the nucleus, including A-, B-, and C-capsids (Figs. 2 & 3A); (2) nucleocapsids budding through the nuclear envelope (Fig. 2); and (3) numerous cytoplasmic vacuoles containing nucleocapsids surrounded by a uniformly staining ellipsoidal tegument layer and a transparent envelope (Fig. 3B,C) (Tandon et al. 2015). The EsHV1 nucleocapsid size, shape, and overall pattern of virion morphogenesis are similar to previous reports (Yamamoto et al. 1984, Margenau et al. 1995, Graham et al. 2004). Although most alloherpesviruses typically generate cytoplas-

Table 3. Phenetic analysis of amino acid (AA) sequences for the partial DNA polymerase and terminase genes (exon 2) among alloherpesviruses. Comparisons of the terminase (97 AA characters including gaps) are above the diagonal and those of the DNA polymerase (164 AA characters including gaps) are below. Values are expressed as a percentage of identity. See Table 2 for virus abbreviations

	RaHV2	RaHV1	AciHV1	CyHV3	CyHV2	CyHV1	AngHV1	SalHV4	SalHV3	SalHV2	SalHV1	IcHV2	IcHV1	AciHV2	EsHV1
RaHV2	–	56.4	52.7	43.0	44.1	43.0	40.9	43.0	43.0	41.9	41.9	42.4	43.5	40.2	39.8
RaHV1	47.8	–	54.8	37.6	38.7	38.7	36.6	40.9	40.9	39.8	39.8	34.8	38.0	34.8	34.4
AciHV1	43.3	44.4	–	46.2	47.3	46.2	47.3	48.9	48.9	47.8	46.7	50.0	48.9	45.7	41.3
CyHV3	41.8	41.0	39.5	–	97.8	95.7	71.0	43.5	43.5	41.3	41.3	39.1	39.1	38.0	37.0
CyHV2	40.3	38.8	40.4	90.3	–	95.7	72.0	43.5	43.5	41.3	41.3	39.1	39.1	38.0	38.0
CyHV1	44.0	43.2	42.2	87.7	86.4	–	69.9	42.4	42.4	40.2	40.2	37.0	37.0	37.0	39.1
AngHV1	41.8	44.7	40.4	64.1	64.1	62.7	–	40.2	40.2	39.1	39.1	40.2	39.1	41.3	37.0
SalHV4	37.2	40.5	45.6	31.0	31.8	31.8	37.2	–	100.0	95.7	95.7	54.3	56.5	54.3	43.0
SalHV3	38.1	39.3	44.6	34.3	31.5	32.9	37.8	95.5	–	95.7	95.7	54.3	56.5	54.3	43.0
SalHV2	41.0	39.6	50.0	36.4	35.7	35.7	40.6	79.5	82.7	–	97.8	53.3	55.4	53.3	43.0
SalHV1	40.3	40.3	45.9	39.1	35.0	35.7	40.6	78.8	82.0	90.7	–	52.2	54.3	52.2	41.9
IcHV2	37.6	36.8	45.9	36.1	34.1	34.1	37.7	60.2	59.6	57.5	57.5	–	96.7	87.0	48.9
IcHV1	36.8	37.6	44.8	35.8	35.5	33.3	39.9	60.2	59.6	58.2	61.6	84.9	–	85.9	48.9
AciHV2	35.1	38.8	48.6	37.4	38.1	38.1	41.5	59.7	61.9	60.5	57.8	73.3	70.5	–	52.2
EsHV1	38.1	38.8	33.3	34.7	38.0	38.0	38.9	45.0	43.8	43.2	45.2	42.8	44.1	44.5	–

mic vacuoles with one to a few virions, the extensive networks of cytoplasmic vacuoles harboring varying numbers of virions (up to 50 in cross-section) in EsHV1 is distinctive and, surprisingly, resembles reports from marine fishes including Pacific cod (McArn et al. 1978) and turbot (Buchanan & Madeley 1978). Similar large cytoplasmic vacuoles have been described for cytomegalovirus infections in mammals (Bia et al. 1983). Future studies are needed to determine whether alloherpesviruses that induce similar gross, microscopic, and ultrastructural lesions share close genetic relationships.

Although first reported in 1978, no sequence data have appeared to resolve the taxonomic position of esocid herpesvirus 1 (Yamamoto et al. 1984). The EsHV1 genome sequences presented here permitted phenetic and phylogenetic analyses that support its inclusion as a novel species within the family *Alloherpesviridae*. The partial EsHV1 genomic map exhibited an identical gene order and direction to the members of the genus *Ictalurivirus* including *Ictalurid herpesvirus 1* and *2*, and *Acipenserid herpesvirus 2* (Fig. 4) (Doszpoly et al. 2011). The phenetic analysis of the partial DNA-dependent DNA polymerase and terminase genes (exon 2) revealed EsHV1 is a genetically distinct taxon exhibiting greatest amino acid identity to the aforementioned ictaluriviruses and viruses infecting salmonids (i.e. salmoniviruses; Table 3). The phylogenetic analysis based on the partial DNA-dependent DNA polymerase and terminase genes supported EsHV1 as a distinct branch most closely related to the clade composed of the ictaluriviruses and salmoniviruses (Fig. 5). It is interesting that EsHV1 branches near the salmonid alloherpesviruses given esociform and salmoniform fishes are known to be each other's closest relative (Campbell et al. 2013). Future phylodynamic analyses based on a greater portion of the EsHV1 genome may reveal that it, too, has codiversified with its esocid host, as has been reported for some mammalian and fish herpesviruses (McGeoch et al. 2005, Waltzek et al. 2009).

Multiple observations have been made of blue spot disease in wild northern pike across space and time, including Canada from 1978 to 1982 (Yamamoto et al. 1984), the midwest USA from 1984 to 1991 (Margenau et al. 1995), Ireland in 2003 (Graham et al. 2004), and again in the midwest USA in 2014 (this study). Notably, blue spot disease has only been observed in the winter and spring months, from February to May. This time period corresponds to the northern pike spawning season, which occurs during the spring as winter ice melts and temperatures rise

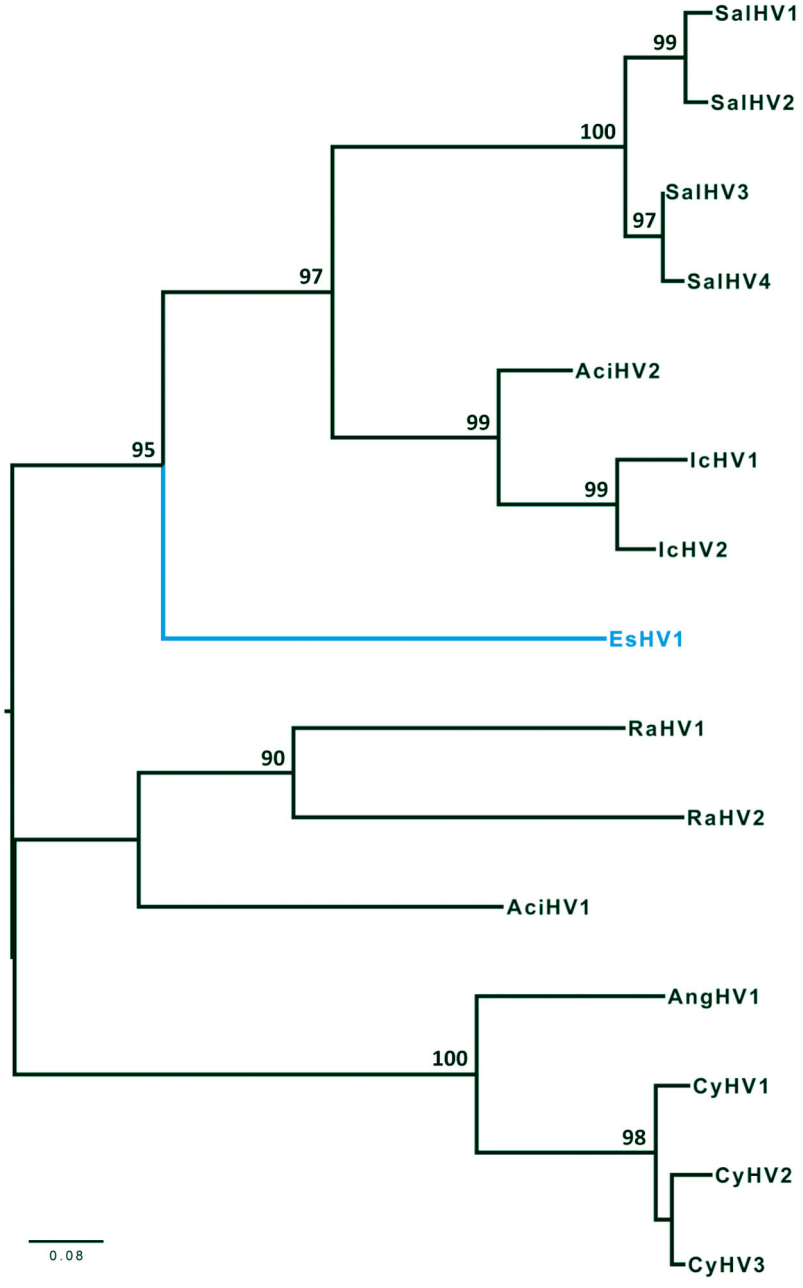

Fig. 5. Phylogram depicting the relationship of esocid herpesvirus 1 (EsHV1) to other alloherpesviruses based on the concatenated partial amino acid (AA) sequences of the DNA-dependent DNA polymerase and terminase (exon 2) genes (261 AA characters including gaps). The maximum likelihood tree was created using 1000 bootstraps with values >70 included above each node. Branch lengths are based on the number of inferred substitutions, as indicated by the scale bar. See Table 2 for virus abbreviations

above 2°C (Margenau et al. 1995). As northern pike aggregate for spawning, behaviors associated with reproduction involve close contact and can result in epidermal injury (Becker 1983). Furthermore, endocrinological changes associated with reproduction have been shown to depress host immunocompetence through decreased lymphocyte activity (Anders & Yoshimizu 1994). Northern pike immunocompetence may also decrease with the seasonal drop in water temperature, predisposing them to blue spot disease, as has been described in common carp infected with CyHV1. The hyperplastic cutaneous lesions induced by CyHV1 in common carp varieties occurs seasonally as water temperatures decline below 20°C (Wolf 1988). When water temperatures rise again, the skin growths spontaneously regress, likely due to a strong cell-mediated response, as leukocytes are abundant in resolving skin lesions (Morita & Sano 1990, Sano et al. 1993). The appearance of herpesviral induced proliferative skin lesions during spring spawning aggregations has also been reported in walleye (Bowser et al. 1988), European smelt (Anders & Möller 1985), and rainbow smelt (Herman et al. 1997). Thus, the replication strategy of EsHV1 and other alloherpesviruses has likely evolved to exploit host life history characteristics that ensure viral host transmission.

In this investigation we genetically characterized a novel alloherpesvirus from northern pike with signs of blue spot disease. The gross, microscopic, and ultrastructural pathology described in our case was identical to previous reports of blue spot disease in northern pike and muskellunge. Phenetic and phylogenetic analyses confirmed that EsHV1 forms a distinct branch among alloherpesviruses. Thus, we propose the formal species designation of *Esocid herpesvirus 1* to be considered for approval by the ICTV. Future studies are needed to determine whether genetic variation exists between EsHV1 from disparate geographical regions (e.g. North American versus European northern pike) or a different esocid host (e.g. muskellunge). Finally, the isolation of EsHV1 is needed to both confirm its role in blue spot disease and facilitate the sequencing of the viral genome to elucidate the molecular mechanisms by which EsHV1 induces epithelial proliferation.

Acknowledgements. We thank T. M. Patrick, M. Gotesman, and R. Alvarado for their technical assistance throughout the study.

LITERATURE CITED

Altschul SF, Madden TL, Schaffer AA, Zhang J, Zhang Z, Miller W, Lipman DJ (1997) Gapped BLAST and PSI-BLAST: a new generation of protein database search programs. Nucleic Acids Res 25:3389–3402

Amin OM (1979) Lymphocystis disease in Wisconsin. J Fish Dis 2:207–217

Anders K, Möller H (1985) Spawning papillomatosis of smelt, *Osmerus eperlanus* L., from the Elbe estuary. J Fish Dis 8:233–235

Anders K, Yoshimizu M (1994) Role of viruses in the induction of skin tumours and tumour-like proliferations of fish. Dis Aquat Org 19:215–232

Becker GC (1983) Fishes of Wisconsin. University of Wisconsin Press, Madison, WI

Békési L, Kovács-Gayer E, Rátz F, Turkovics O (1984) Skin infection of the sheatfish (*Siluris glanis* L.) caused by a herpes virus. In: Olah J (ed) Symposia biologica Hungarica 23. Akadémiai Kiadó, Budapest, p 25–30

Bia FJ, Griffith BP, Fong CKY, Hsiung GD (1983) Cytomegaloviral infections in the guinea pig: experimental models for human disease. Clin Infect Dis 5:177–195

Bowser PR, Wolfe MJ, Forney JL, Wooster GA (1988) Seasonal prevalence of skin tumors from walleye (*Stizostedion vitreum*) from Oneida Lake, New York. J Wildl Dis 24:292–298

Buchanan JS, Madeley CR (1978) Studies on *Herpesvirus scophthalmi* infection of turbot *Scophthalmus maxiumus* (L.) ultrastructural observations. J Fish Dis 1: 283–295

Buchanan JS, Richards RH, Sommerville C, Madeley CR (1978) A herpes-type virus from the turbot, *Scophthalmus maximus*, L. Vet Rec 102:527–528

Campbell MA, López JA, Sado T, Miya M (2013) Pike and salmon as sister taxa: detailed intraclade resolution and divergence time estimation of Esociformes + Salmoniformes based on whole mitochondrial genome sequences. Gene 530:57–65

Craig JF (2008) A short review of pike ecology. Hydrobiologia 601:5–16

Craig JF (ed) (2013) Pike: biology and exploitation, Vol 19. Springer Science & Business Media, Dordrecht

Davison AJ (1998) The genome of *Salmonid herpesvirus 1*. J Virol 72:1974–1982

Davison AJ, Eberle R, Ehlers B, Hayward GS and others (2009) The order *Herpesvirales.* Arch Virol 154:171–177

Davison AJ, Kurobe T, Gatherer D, Cunningham C and others (2013) Comparative genomics of carp herpesviruses. J Virol 87:2908–2922

de Kinkelin P, Galimard B, Bootsma R (1973) Isolation and identification of the causative agent of 'red disease' of pike (*Esox lucius* L. 1766). Nature 241:465–467

Doszpoly A, Shchelkunov I (2010) Partial genome analysis of Siberian sturgeon alloherpesvirus suggests its closest relation to AciHV2. Acta Vet Hung 58:269–274

Doszpoly A, Benk M, Bovo G, LaPatra SE, Harrach B (2011) Comparative analysis of a conserved gene block from the genome of the members of the genus *Ictalurivirus.* Intervirology 54:282–289

Enzmann PJ, Konrad M, Parey K (1993) VHS in wild living fish and experimental transmission of the virus. Fish Res 17:153–161

Faisal M, Shavalier M, Kim KK, Millard EV and others (2012) Spread of emerging viral hemorrhagic septicemia virus strain, genotype IVb, in Michigan, USA. Viruses 4: 734–760

FAO (Food and Agriculture Organization of the United Nations) (2015) *Esox lucius* fact sheet. www.fao.org/fishery/species/2942/en (accessed 8 Sep 2015)

Graham DA, Curran WL, Geoghegan F, McKiernan F, Foyle KL (2004) First observation of herpes-like virus particles in northern pike, *Esox lucius* L., associated with bluespot-like disease in Ireland. J Fish Dis 27:543–549

Hanson LA, Rudis MR, Vasquez-Lee M, Montgomery RD (2006) A broadly applicable method to characterize large DNA viruses and adenoviruses based on the DNA polymerase gene. Virol J 3:28

Hellberg H, Koppang EO, Tørud B, Bjerkås I (2002) Subclinical herpesvirus infection in farmed turbot *Scophthalmus maximus*. Dis Aquat Org 49:27–31

Herman RL, Burke CN, Perry S (1997) Epidermal tumors of rainbow smelt with associated virus. J Wildl Dis 33: 925–929

Humason GL (1979) Animal tissue techniques, 4th edn. WH Freeman & Co, San Francisco, CA

Iida Y, Masumura K, Nakai T, Sorimachi M, Matsuda H (1989) A viral disease in larvae and juveniles of the Japanese flounder *Paralichthys olivaceus.* J Aquat Anim Health 1:7–12

Katoh K, Kuma K, Toh H, Miyata T (2005) MAAFT version 5: improvement in accuracy of multiple sequence alignment. Nucleic Acids Res 33:511–518

Kelly RK, Nielsen O, Mitchell SC, Yamamoto T (1983) Characterization of *Herpesvirus vitreum* isolated from hyperplastic epidermal tissue of walleye, *Stizostedion vitreum vitreum* (Mitchell). J Fish Dis 6:249–260

Marcos-Lopez M, Waltzek TB, Hedrick RP, Baxa DV and others (2012) Characterization of a novel alloherpesvirus from Atlantic cod (*Gadus morhua*). J Vet Diagn Invest 24: 65–73

Margenau TL, Marcquenski SV, Rasmussen PW, MacConnell E (1995) Prevalence of blue spot disease (esocid herpesvirus-1) on northern pike and muskellunge in Wisconsin. J Aquat Anim Health 7:29–33

McAllister PE, Lidgerding BC, Herman RL, Hoyer LC, Hankins J (1985) Viral diseases of fish: first report of carp pox in golden ide (*Leuciscus idus*) in North America. J Wildl Dis 21:199–204

McArn GE, McCain B, Wellings SR (1978) Skin lesions and associated virus in Pacific cod (*Gadus macrocephalus*) in the Bering Sea. Fed Proc 37:937

McGeoch DJ, Gatherer D, Dolan D (2005) On phylogenetic relationships among major lineages of the *Gammaherpesvirinae.* J Gen Virol 86:307–316

Meier W, Jørgensen PEV (1980) Isolation of VHS virus from pike fry (*Esox lucius*) with haemorrhagic symptoms. In: Ahne W (ed) Fish diseases. Springer-Verlag, Berlin, p 8–17

Morita N, Sano T (1990) Regression effect of carp, *Cyprinus carpio* L, peripheral blood lymphocytes on CHV-induced carp papilloma. J Fish Dis 13:505–511

Morrison CM, Leggiadro CT, Martell DJ (1996) Visualization of viruses in tumors of rainbow smelt *Osmerus mordax*. Dis Aquat Org 26:19–23

Muhire BM, Varsani A, Martin DP (2014) SDT: a virus classification tool based on pairwise sequence alignment and identity calculation. PLOS ONE 9:e108277

Richards RH, Buchanan JS (1978) Studies on *Herpesvirus scophthalmi* infection of turbot *Scophthalmus maximus*: histopathological observations. J Fish Dis 1:251–258

Sano N, Moriwake M, Sano T (1993) Herpesvirus cyprini: thermal effects on pathogenicity and oncogenicity. Fish Pathol 28:171–175

Shchelkunov IS, Karaseva TA, Kadoshnikov YUP (1992) Atlantic salmon papillomatosis: visualization of herpesvirus-like particles in skin growths of affected fish. Bull Eur Assoc Fish Pathol 12:28–31

Tandon R, Mocarski ES, Conway JF (2015) The A, B, Cs of herpesvirus capsids. Viruses 7:899–914

Waltzek TB, Kelley GO, Alfaro ME, Kurobe T, Davison AJ, Hedrick RP (2009) Phylogenetic relationships in the family *Alloherpesviridae.* Dis Aquat Org 84:179–194

Wolf K (1988) Fish viruses and fish viral diseases. Cornell University Press, Ithaca, NY

Wolke RE, Murchelano RA (1976) A case report of an epidermal papilloma in *Mustelus canis.* J Wildl Dis 12: 167–171

Yamamoto T, Kelly RK, Nielsen O (1984) Epidermal hyperplasias of northern pike (*Esox lucius*) associated with herpesvirus and C-type particles. Arch Virol 79:255–272

Editorial responsibility: Mark Crane, Geelong, Victoria, Australia

Submitted: June 28, 2016; Accepted: August 30, 2016
Proofs received from author(s): November 8, 2016